Measurement of ligand distribution in individual adsorbent particles using confocal scanning laser microscopy and confocal micro-Raman spectroscopy

ARTICLE *in* JOURNAL OF CHROMATOGRAPHY A · NOVEMBER 2000

Impact Factor: 4.17 · DOI: 10.1016/S0021-9673(00)00684-1 · Source: PubMed

4 AUTHORS, INCLUDING:

Anders Ljunglöf
General Electric
14 PUBLICATIONS **701** CITATIONS

SEE PROFILE

ELSEVIER

Journal of Chromatography A, 893 (2000) 235–244

JOURNAL OF CHROMATOGRAPHY A

www.elsevier.com/locate/chroma

Measurement of ligand distribution in individual adsorbent particles using confocal scanning laser microscopy and confocal micro-Raman spectroscopy

Anders Ljunglöf[a,*], Mina Larsson[b], Karl-Gustav Knuuttila[a], Jan Lindgren[b]

[a] *Amersham Pharmacia Biotech, Björkgatan 30, SE-75184 Uppsala, Sweden*

[b] *Uppsala University, The Ångström Laboratory, Inorganic Chemistry, Box 538, SE-751 21 Uppsala, Sweden*

Received 13 April 2000; received in revised form 15 June 2000; accepted 16 June 2000

Abstract

Two methods, confocal scanning laser microscopy and confocal micro-Raman spectroscopy were used to analyse the distribution of IgG antibodies immobilized on CNBr-activated agarose beads. In the first method the internal distribution profile of fluorescent labelled Protein A was used as an indirect measure of the distribution of IgG, while the second method detects vibrations originating from aromatic amino acids present in the immobilized antibodies. Both these methods indicate an homogeneous ligand distribution within IgG Sepharose 4 Fast Flow and IgG Sepharose 6 Fast Flow.

Keywords: Affinity adsorbents; Confocal scanning laser microscopy; Confocal micro-Raman spectroscopy; Agarose beads; Immobilized proteins; Stationary phase, LC; Immunoglobulins

1. Introduction

Affinity chromatography media are generally composed of a hydrophilic, neutral and macroporous matrix that contains functional groups to which a specific ligand is attached. Generally, ligands may be classified as either mono-specific or group-specific [1,2]. The group-specific ligands have affinity for a group of related substances. One example of this kind of ligand is Protein A, a receptor protein with primary binding activity restricted to the Fc region of immunoglobulin G [3,4]. Mono-specific ligands bind to a very small number of solutes. Examples include lysine which binds plasminogen from blood plasma [5], and avidine which binds biotin [6]. Antibodies have very high specificity and have become very popular as ligands. This type of affinity medium is called an immunosorbent. Purification factors of several thousand-fold with more than 90% recovery may be achieved in a single step [1].

In general, the immobilization of a ligand consists of three steps: activation of the matrix to make it reactive towards the functional group of the ligand, coupling of the ligand, and deactivation and blocking of residual active groups. The commonly used technique for activation of affinity adsorbents is the

*Corresponding author.

E-mail address: anders.ljunglof@eu.apbiotech.com (A. Ljunglöf).

0021-9673/00/$ – see front matter
PII: S0021-9673(00)00684-1

CNBr method, originally developed by Axén and co-workers [7,8]. An overview of various immobilization methods is given in reference [1].

One issue of great interest is knowledge about the resulting ligand distribution in the chromatographic matrices. For this purpose, methods for direct measurement of ligand distribution in individual adsorbent particles are desirable. One way of obtaining images with sufficient resolution is to use mechanical sectioning with a microtome. Fluorescently labelled proteins can then be visualized by fluorescence microscopy [9,10]. Another approach is to use autoradiography to record the spatial distribution of radioisotopes within the specimen. Autoradiographs can be obtained by exposing photosensitive films to the γ radiation from adsorbed ^{125}I-labelled protein [11]. However, both mechanical sectioning and autoradiography are quite laborious and time-consuming.

In this study, two alternative techniques i.e. confocal scanning laser microscopy (CSLM) and confocal micro-Raman spectroscopy were used to analyse the distribution of IgG immobilized on CNBr activated Sepharose. CSLM has previously been shown to be a useful tool for studying protein and DNA adsorption to single chromatography adsorbent particles [12–17]. In brief, emitted fluorescent light orginating from a solute labelled with a fluorescent dye, is allowed to pass through a pinhole aperture positioned in front of a detector (i.e. photomultiplier tube). The pinhole aperture effectively blocks light from out-of-focus-planes. This depth discriminating property makes it possible to slice the specimen optically into thin sections [18–20]. The principles and applications of confocal microscopy have been extensively described in the literature [21,22]. Confocal micro-Raman spectroscopy combines the chemical information from vibrational spectroscopy with the spatial resolution of confocal microscopy [23,24]. Depth profiles or lateral Raman mappings can be recorded by moving the sample through the focus of the microscope objective. In this way it is possible to monitor the distribution of different components of a specimen. Such Raman mapping can give proof of homogeneous or inhomogeneous mixtures without additional staining or other complicated sample preparations [25].

2. Experimental

2.1. Instrumentation

Confocal microscopy measurements were performed with a Leica TCS SP confocal scanning laser microscope equipped with an argon–krypton laser and with TCS NT software for image evaluation. Confocal and non-confocal dispersive micro-Raman spectroscopy was performed with a Renishaw System 2000 micro-Raman spectrometer equipped with a near-infrared diode laser (780 nm, 20 mW). Some of the reference spectra were recorded on a Bruker RFS 100/S Fourier transform (FT) Raman spectrometer.

2.2. Adsorbents, proteins and chemicals.

IgG immobilized on CNBr activated Sepharose 4 Fast Flow and Sepharose 6 Fast Flow (below named IgG Sepharose 4 Fast Flow and IgG Sepharose 6 Fast Flow), native Protein A and Cy5 reactive dye were obtained from Amersham Pharmacia Biotech. Labelling of Protein A with Cy5 was performed according to the standard procedure recommended by the manufacturer. All other chemicals were of analytical grade and were obtained from commercial sources.

2.3. Adsorption of Protein A to IgG sepharose

Protein A labelled with Cy5 was used to visualize immobilized IgG. One ml Protein A–Cy5 (2.5 mg ml^{-1} in 20 m*M* sodium phosphate pH 7.0) was mixed with 125 μl of each gel (settled volume) and was gently mixed end-over-end for 30 min. The reaction vial was then centrifuged and the supernatant was removed. To remove the excess of unbound Protein A–Cy5, the gel was washed three times with phosphate buffer, by repeated dilution, centrifugation and decantation. Individual adsorbent particles were then measured by confocal scanning laser microscopy and analysed as described below. As a control experiment, Protein A–Cy5 adsorption to underivatized adsorbent (i.e. Sepharose 4 Fast Flow and Sepharose 6 Fast Flow) was analysed in the same way. Background fluorescence, resulting from non-

specific adsorption, was found to be negligible (data not shown). Furthermore, the influence of protein concentration was investigated by varying the Protein A content in the fluid phase (0.1–0.8 mg ml^{-1}, in 20 m*M* sodium phosphate, 0.15 *M* NaCl pH 7.0). Incubation was performed for 72 h followed by confocal microscopy analysis as described below.

2.4. Adsorption isotherms

Adsorption isotherms for Protein A on IgG Sepharose 4 Fast Flow and IgG Sepharose 6 Fast Flow were determined using a microtiter plate static method. A series of Protein A solutions (in 20 m*M* sodium phosphate buffer, 0.15 *M* NaCl, pH 7.0), 800 μl each (V_{sys}), having different concentrations (C_{ini}) was dispensed into wells of a 96 deep-well microtiter plate (1.2 ml) using an automated liquid handler. To each well 35 μl of gel plug (V_{gel}) was added and the plate covered with a self sealing lid was gently rotated end-over-end for 10 h. After the incubation, the plate was centrifuged at 1000 rpm for 5 min. The concentration of Protein A in the supernatant (C_{eq}) was measured spectrophotometrically at 280 nm, and the total amount of protein adsorbed per ml gel (Q) was calculated from the following mass balance [Eq. (1)]. The amount of Protein A present in the intraparticle pores was considered neglible (<2%).

$$Q = \frac{V_{sys}}{V_{gel}} \cdot (C_{ini} - C_{eq}) \quad (1)$$

The data obtained were used to estimate parameters in the Langmuir isotherm model [Eq. (2)] using a non-linear least square estimation procedure, were K is the dissociation constant (mg ml^{-1}) and Q_{max} is the maximum capacity (mg ml^{-1} adsorbent). In addition, runs without gel were performed in order to monitor the stability of Protein A upon incubation.

$$Q = \frac{Q_{max} C_{eq}}{K + C_{eq}} \quad (2)$$

2.4.1. Confocal scanning laser microscopy

Individual adsorbent particles were analysed by horizontal scanning (i.e. acquisition of two-dimensional confocal images perpendicular to the optical axis). The distribution of fluorescent molecules through the particles was then obtained by translation of confocal images into fluorescence intensity profiles, which show fluorescence intensity as a function of the radial position within the particle [13–16]. A 63×/1.2 water immersion objective[1] was used for all measurements. The laser provided excitation of Cy5 at 647 nm and the emitted fluorescent light was detected between 660 and 800 nm. To reduce background fluorescence and noise, the images were generated by accumulating 8 scans per image. The image size for all images was 512×512 pixels, and the pixel size 0.49 μm.

2.4.2. Confocal micro-Raman spectroscopy

A 50×/0.75 objective and a diode laser (780 nm, 20 mW) were used for all measurements. Reference spectra of IgG (using FT-Raman), Sepharose 6 Fast Flow (using FT-Raman and dispersive micro-Raman), IgG Sepharose 4 and IgG Sepharose 6 Fast Flow (using dispersive micro-Raman) were first recorded in a non-confocal mode. Spectra were recorded between 400 and 1800 cm^{-1} with a wave number resolution of about 1 cm^{-1}.

Adsorbent particles were placed on a metal plate and were allowed to dry in air for 15 min. The particles (diameters between 25 and 65 μm) were then analysed by depth profiling in confocal mode. The start point for each series of measurements was set when focus was on the surface of the metal plate. The measurements were then performed on individual particles with a step length of about 5 μm. Each series of measurements was started at the bottom of the particle and thereafter an upward stepping, using a motorized stage, was performed. A visual check after each series was made, confirming that the upper surface of the particle was reached. The measuring time for each step was about 10 min. A binning factor of 2 or 4 was used in order to increase the signal-to-noise ratio. In order to further reduce the noise, spectra of top, middle and bottom

[1]The optical depth resolution (R_d) can be approximated by $R_d = (1.4\ n\lambda)/(\text{N.A.})^2$ where N.A. is the numerical aperture of the objective, λ is the wavelength of the detected light and n is the refractive index of the mount medium [18,26]. The set-up in this study gives a theoretical depth resolution of ~1 μm.

of the particles were recorded with longer acquisition times (20 min).

3. Results and discussion

3.1. Confocal microscopy

In accordance with earlier studies [10,13], fluorescent labelled Protein A was used for visualization of IgG immobilized on CNBr activated Sepharose particles (i.e. IgG Sepharose 4 and IgG Sepharose 6 Fast Flow). The adsorbent particles were analysed by acquisition of two-dimensional confocal images, and the internal distribution profile of Protein A was then used as an indirect measure of the distribution of IgG. Fig. 1 shows a confocal image and the corresponding intensity profile obtained with IgG Sepharose 4 Fast Flow. As can be seen, the intensity profile is totally uniform. Corresponding results obtained from four IgG Sepharose 6 Fast Flow particles with different particle diameters (45–145 μm) are shown in Fig. 2. Here too, the intensity profiles are uniform irrespective of particle size. These results indicate an even distribution of immobilized antibodies within both Sepharose 4 Fast Flow and Sepharose 6 Fast Flow particles. It can be noted that the maximum fluorescence intensity, obtained by scanning in the middle of individual particles, decreases with increasing particle size (Fig. 2). This darkening has been reported earlier as an effect of light attenuation within the particles [13,27,28].

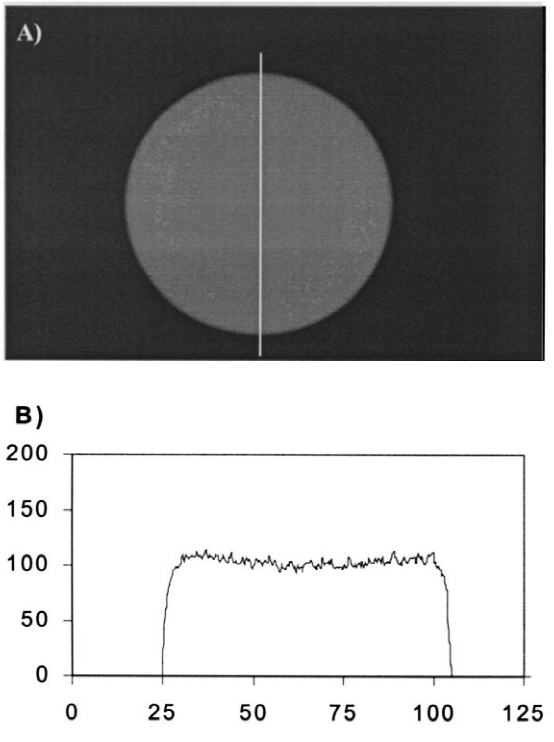

Fig. 1. Confocal image and intensity profile obtained from IgG Sepharose 4 Fast Flow incubated with Protein A–Cy5. (A) Confocal image. The broken line shows the area that was evaluated. (B) Fluorescence intensity profile: *x*-axis shows *xy*-position [μm] within the particle and *y*-axis fluorescence intensity [units].

The influence of protein concentration was investigated by determining the adsorption isotherms for Protein A (Fig. 3). Furthermore, adsorbent particles incubated with varying Protein A concentration were analysed with confocal microscopy. The intensity profiles obtained with IgG Sepharose 4 Fast Flow are shown in Fig. 4. The result reveal that a Protein A concentration below the saturated part of the isotherm results in an inhomogeneous adsorption to the particles. The same effect could also be seen with IgG Sepharose 6 Fast Flow (data not shown). Thus, for indirect measurement of ligand distribution through adsorption of fluorescently labelled molecules, it is very important to make sure that the fluid phase concentration is sufficient for saturation of the whole particles.

3.2. Confocal micro-Raman spectroscopy

Reference spectra for IgG and Sepharose 6 Fast Flow are shown in Fig. 5, and a comparison of spectra obtained with Sepharose 6, IgG Sepharose 4 and IgG Sepharose 6 Fast Flow is shown in Fig. 6. The band at 1670 cm^{-1} is consistent with the amide–I peptide band (not fully resolved from the C–C stretching band), and the band at 1003 cm^{-1} was assigned to in-plane ring deformation originating from the aromatic amino acid phenylalanine present in IgG [29]. These bands can be used to follow the depth distribution of the IgG constituent. To produce depth distribution profiles, a normalisation procedure was performed, whereby the ratio of the intensity of the 1003 cm^{-1} IgG band to the intensity of the 1082

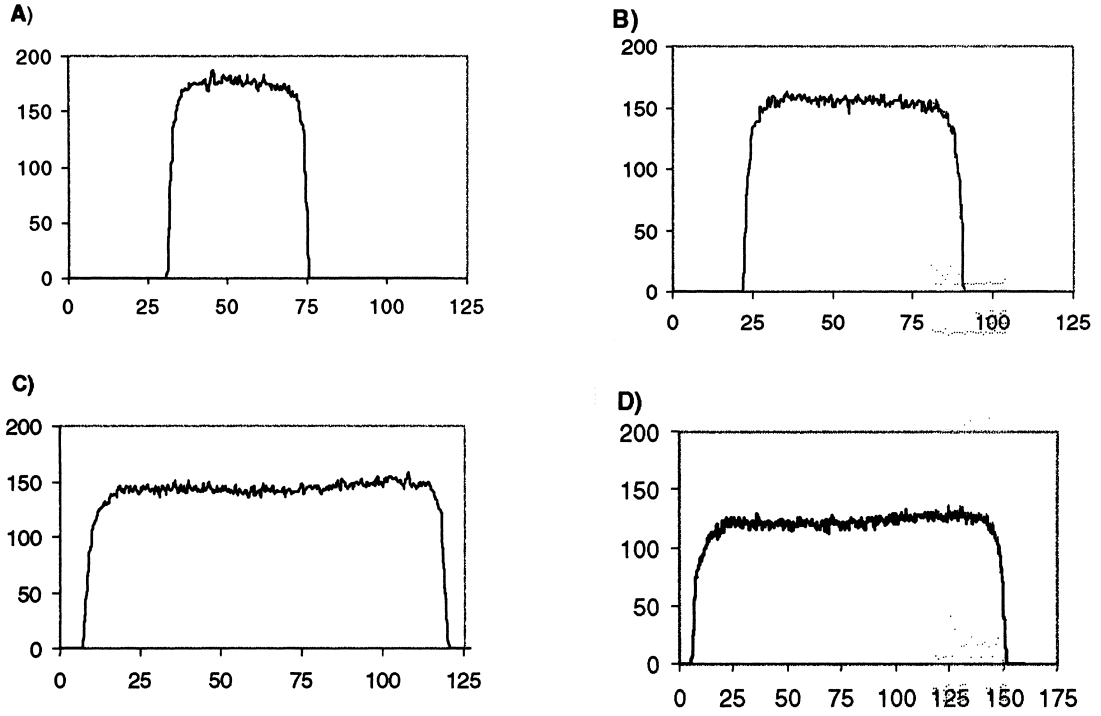

Fig. 2. Fluorescence intensity profiles obtained from IgG Sepharose 6 Fast Flow. Particle size (A) 45 μm, (B) 70 μm, (C) 110 μm, (D) 145 μm. *x*-axis: *xy*-position [μm], *y*-axis: fluorescence intensity [units].

cm^{-1} Sepharose band was calculated. This normalisation served two purposes. First variation in intensity within a particle, due to a varying path length of the beam through the particle, could be removed. Secondly, and for the same reason, intensity variations between particles of different sizes could also be removed. This meant that it was possible to display the results from different particles overlaid in diagrams on a common scale. Results obtained with IgG Sepharose 4 Fast Flow and IgG Sepharose 6 Fast Flow are shown in Figs. 7 and 8. From these results, the noise level can be estimated to ±5% of the measured signal ratio. Fig. 9 shows measurements at the top, middle and bottom of a particle, using longer acquisition times in order to reduce the noise level.

Since the distribution profiles are based on observation of Raman bands originating from IgG itself, these profiles will provide a direct measure of the distribution of IgG. As can be seen from the intensity profiles (Figs. 7 and 8) the distribution of IgG is totally uniform within the particles irrespective of particle size. Moreover, it is seen that the relative amount of IgG and Sepharose is the same for different particle sizes.

4. Conclusions

The present work demonstrates the strength of confocal scanning for measurement of ligand distribution within individual adsorbent particles. Two independent methods, i.e. confocal scanning laser microscopy and confocal micro-Raman spectroscopy, were used to analyse the distribution of IgG immobilized on CNBr activated agarose beads. Both these measurement methods indicate an even distribution of immobilized antibodies within Sepharose 4 Fast Flow and Sepharose 6 Fast Flow.

While CSLM gives an indirect measure through Protein A labelling, confocal micro-Raman spectroscopy detects vibrations originating directly from the immobilized antibodies. The advantage of the latter method is that no sample preparation is

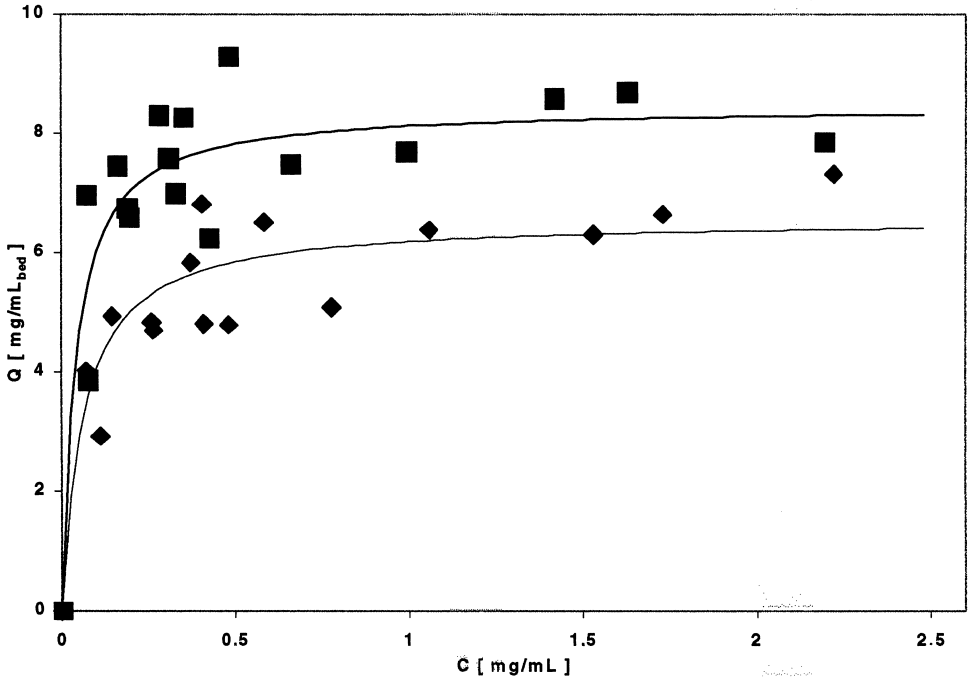

Fig. 3. Adsorption isotherms for Protein A on IgG Sepharose 4 Fast Flow (diamonds) and IgG Sepharose 6 Fast Flow IgG (squares). Lines represent the best fit model predictions obtained with the following values of parameter: IgG Sepharose 4 Fast Flow: $Q_{max}=6.5$ mg ml^{-1} gel, $K=0.06$ mg ml^{-1}; IgG Sepharose 6 Fast Flow: $Q_{max}=8.4$ mg ml^{-1} gel, $K=0.04$ mg ml^{-1}.

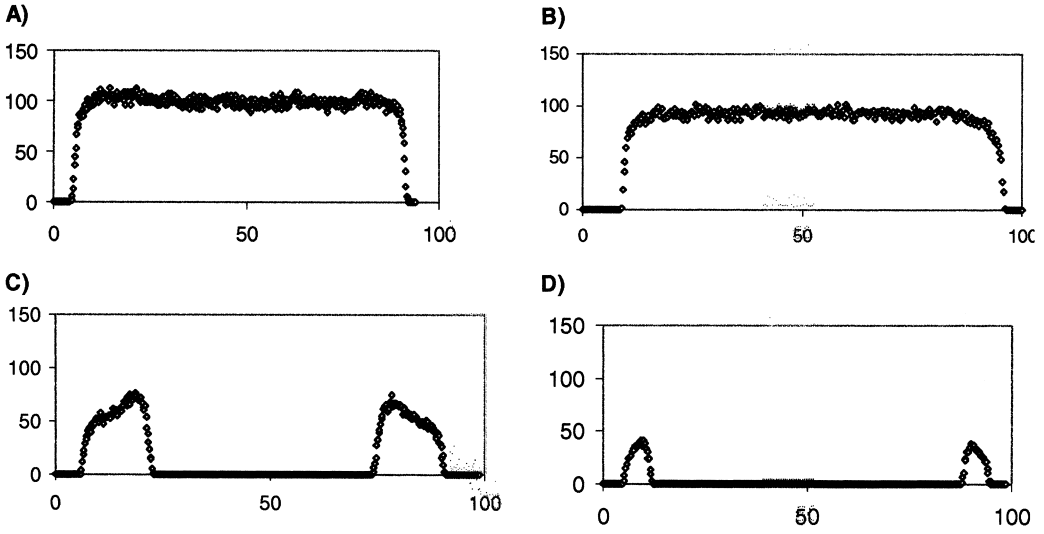

Fig. 4. Fluorescence intensity profiles obtained from IgG Sepharose 4 Fast Flow after incubation with varying fluid phase concentrations. (A) 0.8, (B) 0.4, (C) 0.2, and (D) 0.1 mg Protein A ml^{-1}. *x*-axis: *xy*-position [μm], *y*-axis: fluorescence intensity [units].

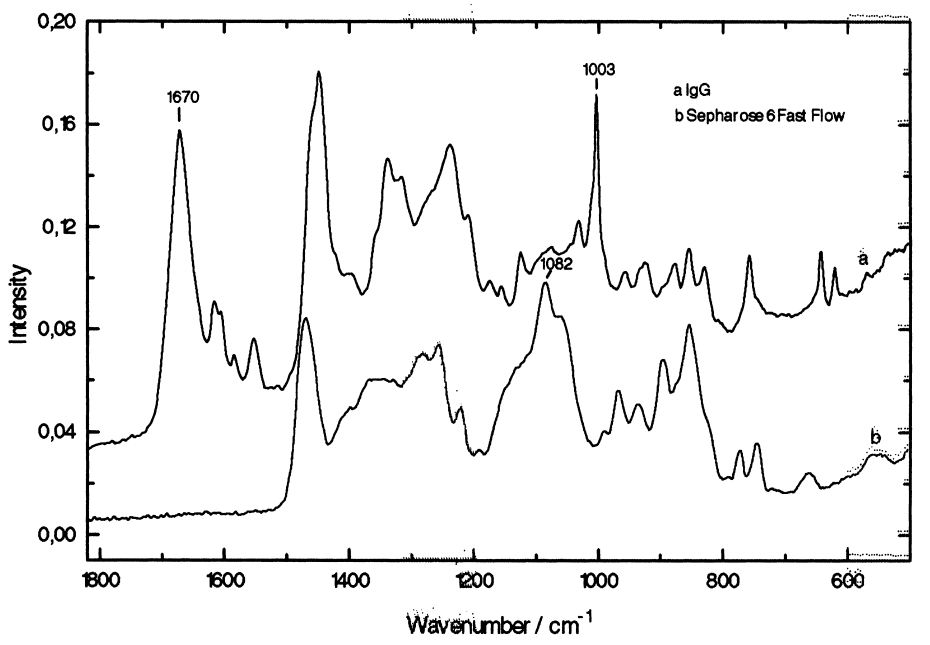

Fig. 5. Reference Raman spectra of IgG and Sepharose 6 Fast Flow, in a capillary tube and as a pellet respectively.

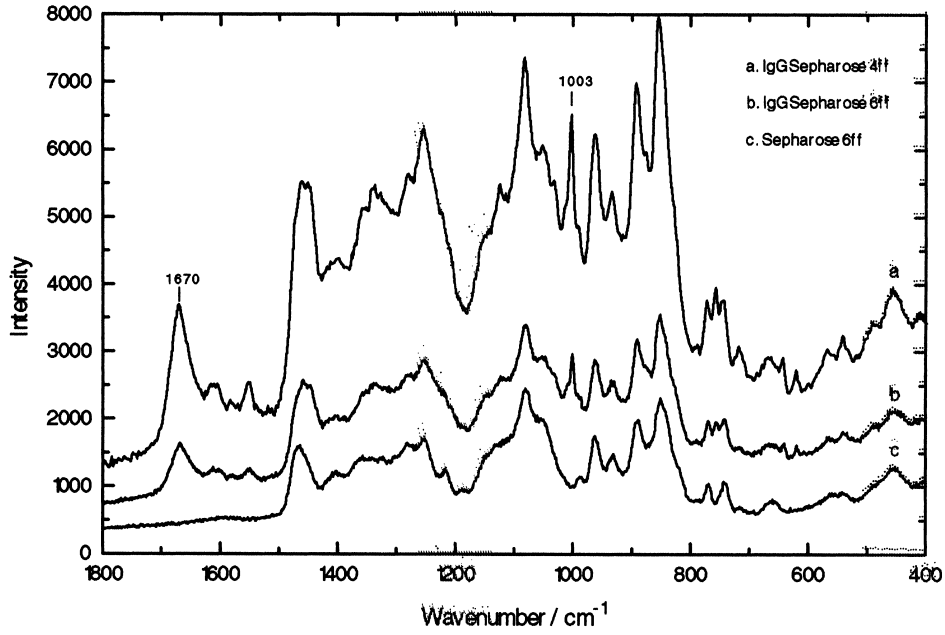

Fig. 6. Reference Raman spectra of IgG Sepharose 4 Fast Flow, IgG Sepharose 6 Fast Flow and Sepharose 6 Fast Flow particles using non-confocal mode.

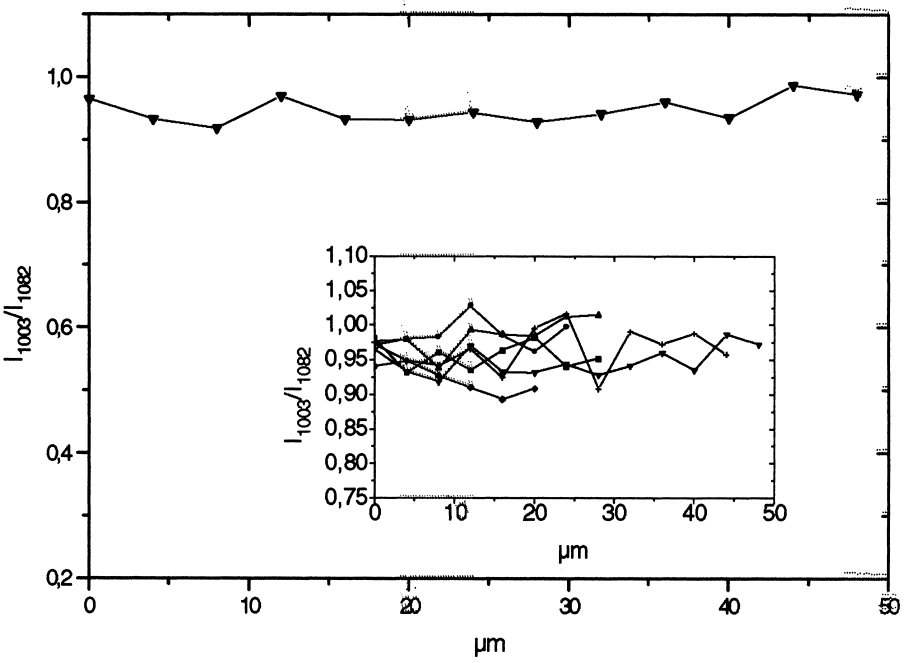

Fig. 7. Intensity ratio of the 1003 cm^{-1} band (from IgG) and the 1082 cm^{-1} band (from Sepharose 4 Fast Flow) as a function of the position in a particle where 0 refers to the bottom and the other points to different heights in µm relative to the bottom. Insert: Intensity ratios for 6 different particles of different diameters.

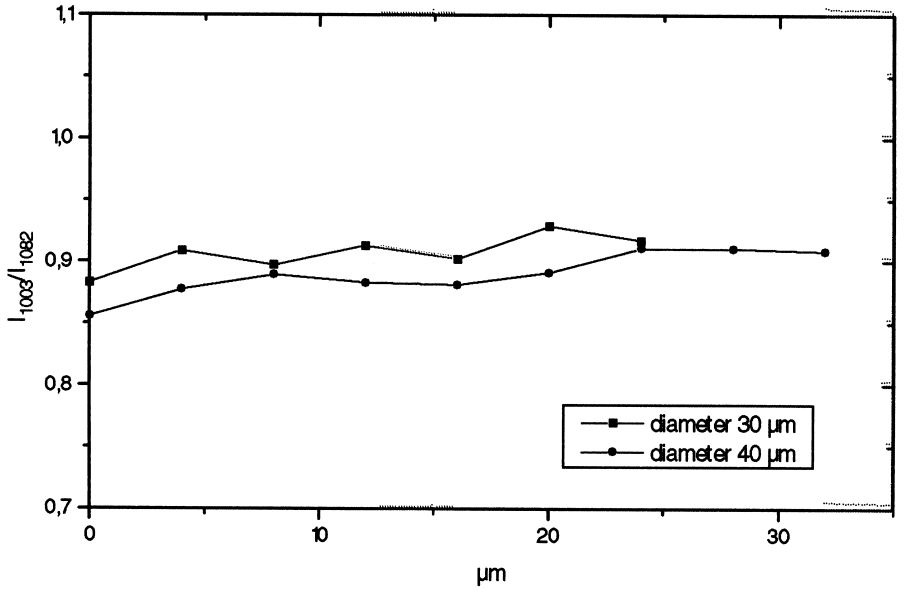

Fig. 8. Intensity ratio of the 1003 cm^{-1} band of IgG and the 1082 cm^{-1} band of Sepharose 6 Fast Flow as a function of the position in a particle where 0 refers to the bottom and the other points to different heights in µm relative to the bottom.

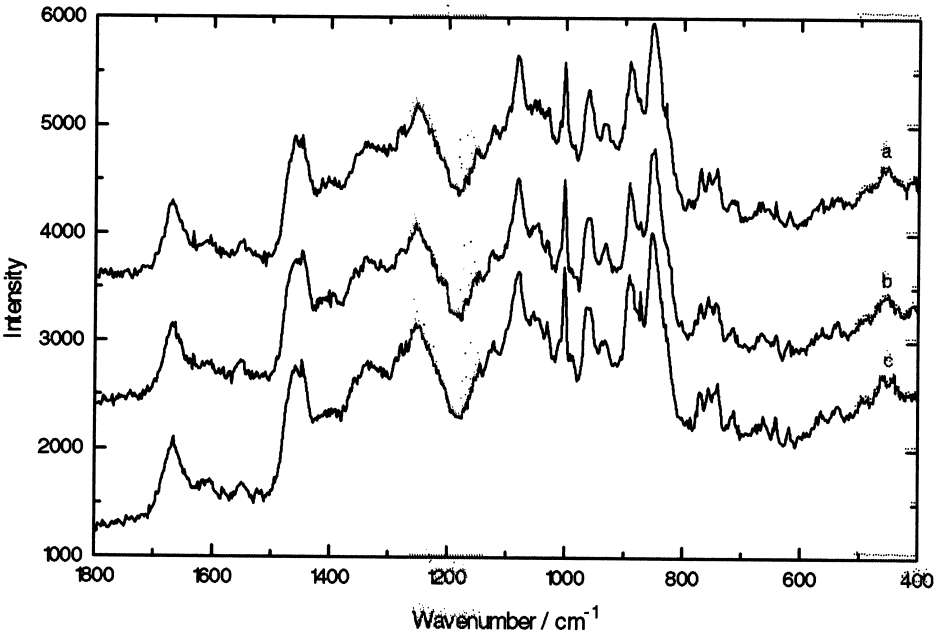

Fig. 9. Raman spectra for a single IgG Sepharose 4 Fast Flow particle measured at the (a) top, (b) middle, and (c) bottom.

required. However, the measurement times are longer and the sensitivity is lower. Furthermore, for direct measurement with Raman spectroscopy it is necessary to identify a significant band originating from the ligand, that gives a sufficiently strong signal in relation to the base matrix.

Recently, it was reported that coupling of anti-factor VIII antibodies to pre-activated Sepharose 4 Fast Flow, resulted in an uneven ligand distribution within the agarose beads [10]. As described above, a fluorescent Protein A conjugate was incubated with adsorbent particles (100 μl of 0.12 mg Protein A ml^{-1} to 10 μl gel suspended in 300 μl buffer). Images were then recorded with a charge-coupled device (CCD) camera attached to a fluorescence microscope. The result indicated a higher ligand density at the surface of the beads. However, the results in this study shows that the observed ligand profile assymetry probably[2] is an effect of incomplete saturation during incubation with Protein A. Thus, it is likely that a low fluid phase concentration resulted in inhomogeneous adsorption.

[2]The authors did not have access to Sepharose 4 Fast Flow coupled with anti-factor VIII antibodies.

Acknowledgements

Thanks to Dr. Karol Lacki for providing the adsorption isotherms and Dr. Lars Hagel for critically reviewing the manuscript (both from Amersham Pharmacia Biotech). This work has been supported by grants from the Swedish National Science Research council.

References

[1] J. Carlsson, J.-C. Janson, M. Sparrman, in: J.-C. Jansson, L. Ryden (Eds.), Protein Purification — principles, High Resolution Methods and Applications, Wiley–VCH, New York, 1998, Chapter 5.
[2] G. Sofer, L. Hagel, Handbook of Process Chromatography, Academic Press, London, 1997.
[3] A. Forsgren, J. Sjöquist, J. Immunol. 97 (1966) 822.
[4] J.J. Langone, Adv. Immunol. 32 (1982) 157.
[5] D.G. Deutsch, E.T. Mertz, Science 170 (1970) 1095.
[6] J.V. Babashak, T.M. Phillips, J. Chromatogr. A 444 (1988) 21.
[7] R. Axén, J. Porath, S. Ernback, Nature 214 (1967) 214.
[8] R. Axén, S. Ernback, Eur. J. Biochem. 18 (1971) 351.
[9] A. Subramanian, K.E. Van Cott, D.S. Milbrath, W.H. Velander, J. Chromatogr. A 672 (1994) 11.

[10] E. Pålsson, A.-L. Smeds, A. Petersson, P.-O. Larsson, J. Chromatogr. A 840 (1999) 39.
[11] J. Liu, Dissertation, Department of Material Science and Engineering, University of Utah, 1997.
[12] H.-B. Kim, M. Hayashi, K. Nakatani, N. Kitamura, Anal. Chem. 68 (1996) 409.
[13] A. Ljunglöf, R. Hjorth, J. Chromatogr. A 743 (1996) 75.
[14] A. Ljunglöf, J. Thömmes, J. Chromatogr. A 813 (1998) 387.
[15] M. Ahmed, D.L. Pyle, J. Chem. Biotechnol. 74 (1999) 193.
[16] A. Ljunglöf, P. Bergvall, R. Bhikhabhai, R. Hjort, J. Chromatogr. A 844 (1999) 129.
[17] T. Linden, A. Ljunglöf, M.-R. Kula, J. Thömmes, Biotechnol. Bioeng. 65 (1999) 622.
[18] K. Carlsson, N. Åslund, Appl. Opt. 26 (1987) 3232.
[19] K. Carlsson, P.E. Danielsson, R. Lenz, A. Liljeborg, L. Majlöf, N. Åslund, Opt. Lett. 10 (1985) 53.
[20] T. Wilson, J. Microscopy 152 (2) (1989) 143.
[21] T. Wilson (Ed.), Confocal Microscopy, Academic Press, San Diego, 1990.
[22] J.B. Pawley (Ed.), Handbook of Biological Confocal Microscopy, Plenum Press, New York, 1995.
[23] J.T. Ferraro, K. Nakamoto, Introductory To Raman Spectroscopy, Academic Press, San Diego, CA, 1994.
[24] G. Turrell, P. Dhamelincourt, in: J.J. Laserna (Ed.), Modern Techniques in Raman Spectroscopy, Wiley, Chichester, 1996.
[25] W. Schrof, J. Klinger, W. Heckmann, D. Horn, Colloid Polym. Sci. 276 (1998) 577.
[26] L. Majlöf, P.-O. Forsgren, in: B. Matsumoto (Ed.), Methods in Cell Biology, Vol. 38, Academic Press, 1993, p. 79.
[27] A. Liljeborg, Three Dimensional Microscopy. Image Acquisition and Processing, II. Proceedings SPIE 2655 (1996) 11.
[28] M. Malmsten, K. Xing, A. Ljunglöf, J. Colloid Interf. Sci. 220 (2) (1999) 436.
[29] S.F. Altschul, T.L. Madden, A.A. Schäffer, J. Zhang, Z. Zhang, W. Miller, D.J. Lipman, Nucleic Acid Res. 25 (1997) 3389.